

Heat Balance Study on Yala Glacier in Langtang Himal, Nepal

Hiroshi TAKAHARA*, Keiji HIGUCHI* and Dhruba Das MULMI**

Glaciological Expedition of Nepal, Contribution No. 90

**Water Research Institute, Nagoya University, Nagoya 464*

***Department of Meteorology, Trichandra Campus, Tribhuvan University, Kathmandu, Nepal*

Abstract

Observations of the heat balance at the glacier surface were carried out during the early post-monsoon season in 1982 near the terminus of Yala Glacier in Langtang Himal, Nepal. On the basis of results from 7 days without passage of synoptic scale disturbances, it is shown that net shortwave radiation provided 83% and sensible heat flux 17%, respectively, of the heat gain in the daytime. Net longwave radiation was found to be a large heat sink. Latent heat flux made no significant contribution to the heat balance. The contribution of sensible heat flux to the daily heat gain was great despite the low air temperature (mean, -3.9°C). Detailed observations revealed that the strong radiation inversion and the resultant katabatic wind play major roles in the enhancement of the large sensible heat flux. It is also indicated that warm air advection from the snow-free area in the daytime has a role in maintaining the large sensible heat flux, especially near the glacier terminus.

1. Introduction

Observations of the heat balance at the glacier surface are important for understanding the mass balance of glaciers and the climatological and hydrological aspects of the areas where the glaciers are located. Most of the previous works on heat exchange at the glacier or snow surface in the Nepal Himalaya have been undertaken in the summer monsoon season in connection with the study of the ablation process (Inoue and Yoshida, 1980; Ohata and Higuchi, 1980).

Under cool meteorological conditions during the post-monsoon season the ablation of glaciers is believed to be small. However, as reported by Yasunari (1980), snow-free areas surrounding glaciers can absorb a substantial part of the incoming radiation due to low surface albedo, acting as a heat source for the atmosphere. There is little information on the thermal influence of such snow-free areas upon the process of heat transfer on glaciers.

Glacio-meteorological observations were attempted in the light of the foregoing from September 27 to October 28 during the post-monsoon season in 1982, near the terminus of Yala (Dakpatsen) Glacier, a small glacier in Langtang Himal, Nepal. The present report describes the observational results of the heat balance at the glacier surface, with special attention to the factors controlling the sensible heat transfer at the surface and the effect of local wind system upon the heat balance.

2. Observation sites

The observations were carried out at Yala Glacier in a valley facing south, in Langtang

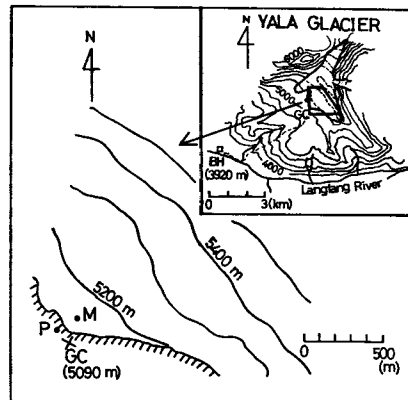


Fig. 1. Map of Yala Glacier and observation sites (M, P and BH). GC: Glacier Camp

Himal, about 60 km north of Kathmandu, Nepal. The topography of the glacier and the surrounding area is shown in Fig. 1. The area of the glacier surface is about 2.6 km². The glacier ice flows from the highest point (5700 m) to the terminus (5100 m) in a southwestward direction.

Micrometeorological observations were carried out at the sites shown in Fig. 1 by M, P and BH. M indicates the micrometeorological observation site (5100 m) on the glacier near the terminus with an average inclination of 8 degrees. The heat balance at the glacier surface was observed at this site at a distance of 70 m from the glacier ice margin in the direction of the prevailing wind. P indicates a point near the 'Glacier Camp' (GC) at the moraine (5090 m), at a distance of 30 m from the glacier terminus. The ground surface is composed mainly of gneiss. BH indicates the low level observation site (3920 m) at the bottom of the wide valley floor of the Langtang River.

3. Methods of observation

At the main observation site M, a mast with instruments was set up on the glacier surface and detailed observations of the wind and temperature profiles were made in order to estimate sensible and latent heat fluxes. Wind speeds were measured at three levels, about 0.6, 1.1 and 2.3 m above the glacier surface by the use of 3-cup type anemometers with a lower limit of 0.2 m·s⁻¹. Air temperatures were measured at 3–5 levels up to 1.9 m with thermistor sensors, shielded by white shelters against radiation, and naturally ventilated. Wet-bulb temperatures were also measured with thermistor sensors covered by wet gauze, and set in the same shelters. The observation of wind direction was made by a wind vane. The glacier surface was covered with snow during the entire observation period. Relative heights of the sensors with respect to the snow surface were measured twice a day, since they changed depending on snowmelt or snowfall. The observation site M is shown in Fig. 2.

Global and reflected solar radiation were measured with pyranometers facing upward and downward, respectively, and the net radiation was measured with a net radiometer.

Other thermistor sensors were set in snow cover or ice at depths of 1, 7, 20, 40 cm in order to estimate the heat used to warm the surface layer. The temperature of the glacier surface was assumed to be equal to that measured at the depth of 1 cm.

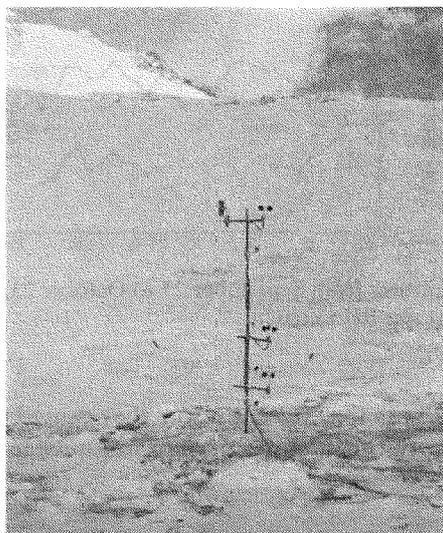


Fig. 2. Photograph of the mast with instruments at site M on the glacier.

These meteorological elements were recorded mainly by a multi-channel chart recorder powered by battery.

Accumulation and ablation were calculated from the snow depth measured by a stake, and the density of snow was measured by a snow sampler. The observations at site M were made for the period from September 27 to October 28 in 1982. The times in the present report are stated in Nepal Standard Time.

At the observation site P at the terminal moraine, measurement of temperature profile up to 1.6 m level was occasionally made with thermistor sensors. At the observation site BH, measurement of air temperature was made at a height of around 1.5 m every hour by the use of a thermistor sensor (Yamada et al., 1984). In addition, precipitation was continuously measured by a simple rain gauge.

4. Meteorological conditions during observation period

4.1. Precipitation and cloud amount

One of the characteristics of the meteorological conditions during the observation period in this area is low precipitation. The total precipitation observed at site BH was about 100 mm in September, but it decreased to about 20 mm in October, indicating the beginning of the post-monsoon season. At the observation site M at the glacier, most of the precipitation was due to synoptic scale disturbances, and fell in the form of snow during the observation period. Contrary to this, nearly all precipitation took the form of rain at the observation site BH. The terrain surrounding the glacier was without snow cover in September, but occasionally there was thin snow cover of less than 20 cm deep in October, when synoptic scale disturbances passed through this area.

The cloud amount observed at site M was low, with a mean value of 4/10 in the daytime. The high cloud amount of more than 8/10 was sometimes observed to be associated with the passage of synoptic scale disturbances or the formation of orographic clouds. Dense oro-

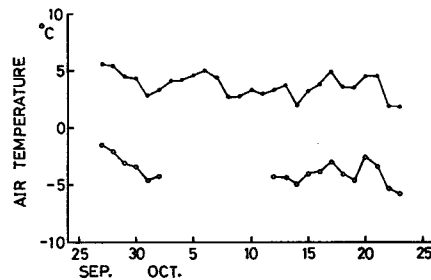


Fig. 3. Daily mean air temperatures from September 27 to October 23. Open circle shows the data at site M (5100 m); solid circle at site BH (3920 m).

graphic clouds were often seen in the afternoon, and they caused the marked reduction of incoming solar radiation. Generally, the cloud amount was quite low at night and in the morning.

4.2. Air temperature

Fig. 3 shows the daily mean air temperature measured at approximately the 1.5 m level at the observation sites BH and M during the period from September 27 to October 23. Similar variation of the daily mean air temperature can be seen at sites BH and M. The average temperature for the whole observation period was 3.7°C at site BH, and -3.9°C at site M, excluding 9 days when data were not available at site M. At site BH air temperature seldom fell below freezing. By contrast, at site M the daily maximum temperature seldom rose above 5°C.

4.3. Wind direction and speed

Fig. 4(a) indicates the frequency distribution of the 3-hourly wind direction at site M based on the data from 21 observation days. The general pattern of the wind direction was nearly always from the S-SW in the daytime and from the NE with the high frequency of more than 80% at nighttime. Such directions correspond to those of the upslope and downslope winds, respectively. The upslope wind usually started to blow at around 09:00 and ended a little after sunset. Such a diurnal variation was pronounced on fine days. Since the general wind was weak during the observation period, such a wind regime can be considered to form part of the mountain-valley wind system developed in this area.

Fig. 4(b) indicates the frequency distribution of 30-minute averaged speed of prevailing winds at 1.1 m level at site M obtained from whole day observations on 16 days. Wind speed was less than 5 m·s⁻¹ throughout most of the observation period, with a mean value of 3.1 m·s⁻¹. It can be seen in Fig. 4(b) that the NE wind speed is much greater than that of the S-SW wind; the former is 3.4 m·s⁻¹ and the latter 2.6 m·s⁻¹ on the average respectively. The great wind speed was usually observed in the early morning of a fine day during the post-monsoon season. Since maximum speed was observed often at a level of 1.0 to 1.5 m above the glacier surface, this wind can be considered as a glacier wind induced by the strong cooling of the air layer near the glacier surface (Hoinkes, 1954, 1955; Munro and Davies, 1977; Ohata and Higuchi, 1979). Difference in speed between the NE wind and the S-SW one was probably due to the fact that such a katabatic wind was superimposed upon the mountain-valley wind, which was from the NE.

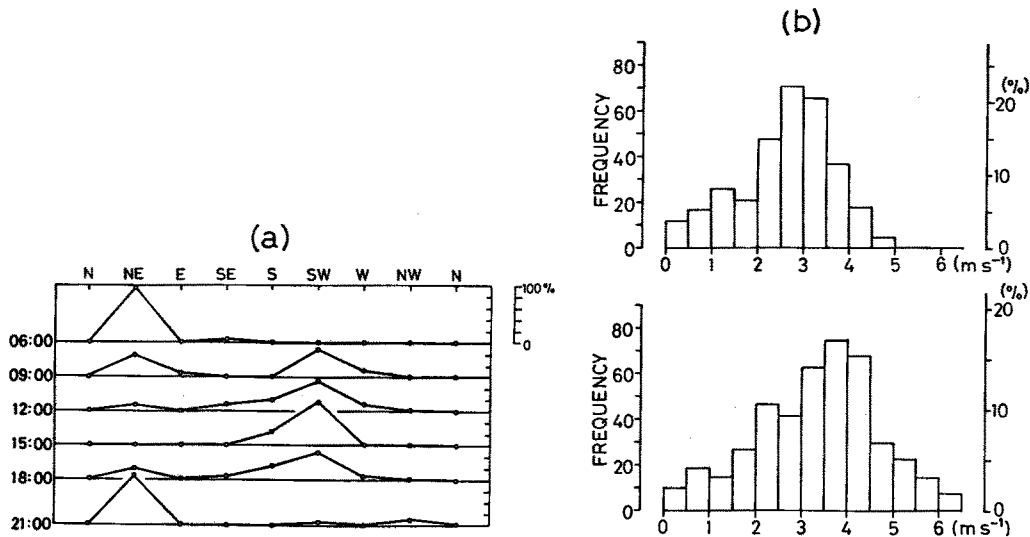


Fig. 4. The frequency distribution of wind direction and wind speed at site M during the post-monsoon season.

(a) 3-hourly wind direction. (b) Wind speed of prevailing winds at 1.1 m level. above: S-SW wind; below: NE wind.

5. Heat balance at glacier surface during post-monsoon season

5.1. Calculation of heat balance components

The heat balance of the surface layer of a glacier can be expressed as follows:

$$Q_S + Q_L + Q_H + Q_E + Q_W + Q_M = 0 \quad (1)$$

where Q_S is the net shortwave radiation, Q_L the net longwave radiation, Q_H the sensible heat flux, Q_E the latent heat flux due to evaporation or sublimation, Q_W the heat used to warm snow and ice of the surface layer and Q_M the heat used to melt snow and ice. Fluxes toward the glacier surface will be defined as positive and those away from the surface as negative. Heat transfer by precipitation was neglected because of its small amount.

(1) Radiation

The net shortwave radiation Q_S was calculated from the global solar radiation and the reflected solar radiation measured independently. The net longwave radiation Q_L can be obtained as a residual from the observed values of Q_S and net radiation $Q_N (= Q_S + Q_L)$.

(2) Sensible and latent heat fluxes

Considering the thermal stratification of the air layer near the glacier surface to be stable, the sensible and latent heat fluxes were calculated by the equations

$$Q_H = \frac{\rho C_p k u_* (T_2 - T_1)}{\phi_H \ln(z_2/z_1)} \quad (2)$$

$$Q_E = \frac{\rho L_{iv} k u_* (q_2 - q_1)}{\phi_E \ln(z_2/z_1)} \quad (3)$$

where ρ is the density of air, C_p the specific heat of air at constant pressure, k von karman's constant, u_* the friction velocity, T the air temperature, L_{iv} the latent heat of evaporation or

sublimation, q the specific humidity, and z the height above the glacier surface. The suffixes 1 and 2 denote two heights where air temperature or specific humidity was measured. Most of the wind profiles were logarithmic, so u_* can be evaluated after logarithmic regression from the wind speed profile. Here ϕ_H and ϕ_E are functions of atmospheric stability, which are related to Obukhov's stability length L by an empirical relation as follows (Webb, 1970):

$$\phi_H = \phi_E = 1 + 5.2 \frac{z}{L} \quad (4)$$

$$L = \frac{\rho C_p u_*^3 \bar{T}}{kg Q_H} \quad (5)$$

where \bar{T} is the temperature representative of the air layer and g is the gravitational acceleration. For simplicity, ϕ_H and ϕ_E are treated as constants independent of z between z_1 and z_2 . Thus Q_H are obtained together with L by solving eqs. (2) and (5) with eq. (4); Q_E are obtained from eqs. (3) and (4) by the use of this L .

To minimize the effect of flux divergence due to advection from the snow-free area, according to fetch criteria established by Bradley (1968) and Rao et al. (1974), z_1 and z_2 were taken as the roughness height (mean, 0.3 cm) and the lowest profile point (within a height of 40 cm), respectively, where the turbulent heat fluxes were considered to be constant with height. This also mitigates the effect of flux divergence arising from the characteristic profile of katabatic wind.

(3) Heat used for warming surface snow and ice layer and melting snow and ice

In most cases the thickness of the overlying snow cover on the glacier ice was 5–20 cm near site M. The heat used to warm snow and ice Q_W was calculated from the time variation of the temperature profile in the surface layer down to a depth of 40 cm, assuming the density of the glacier ice of $0.85 \text{ g}\cdot\text{cm}^{-3}$ and the specific heat of ice of $0.5 \text{ cal}\cdot\text{g}^{-1}\cdot\text{deg}^{-1}$. As for the density of snow, the actual measured value was used.

The heat used in the melting process Q_M was estimated by the direct measurement of the lowering of the snow surface and the density of snow. The free water content was likely to be less than 10% even in the case of melting snow, so it is not taken into account here.

5.2. Daytime heat balance

For the calculation of sensible and latent heat fluxes, 30-minute averaged profiles of wind speed, dry- and wet-bulb temperature were used. Daytime (06:00–18:00) heat balance at the glacier surface was obtained for the periods from September 29 to October 1 and from October 12 to 15. Daily heat balance was estimated during the period from 06:00 on October 12 to 06:00 on October 16, when complete records were obtained. All the observation days were primarily characterized by fine weather conditions and the development of the local wind system. In the afternoon the site M was often covered with orographic clouds; however, synoptic scale disturbances rarely came to this area. Hence, these periods can be considered as representative of the post-monsoon season. The glacier surface near the site M was covered with snow 5–20 cm in depth, but the ground near the glacier terminus was free from snow.

Components of heat balance in the daytime are shown diagrammatically in Fig. 5. The mean values of components of heat balance in the daytime for the 7 days are summarized in Table 1, together with those values of daily heat balance for the period from October 12 to 16. It can be clearly seen in Fig. 5 that the predominant component of heat gain is net shortwave radiation Q_S , which amounts to 83% of the heat gain on the average, followed

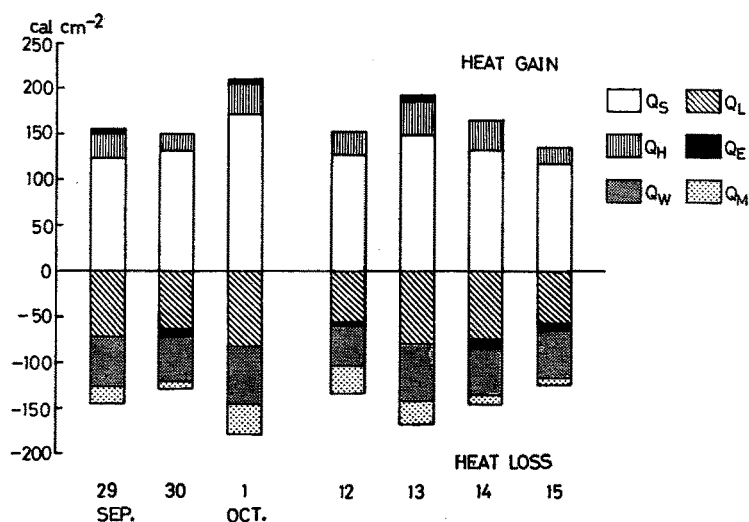


Fig. 5. Daytime heat balance at the glacier surface.

Q_S : net shortwave radiation; Q_L : net longwave radiation; Q_H : sensible heat flux; Q_E : latent heat flux; Q_W : heat used to warm snow and ice; Q_M : heat used to melt snow and ice.

by the sensible heat flux Q_H (17%). The surface albedo at midday ranged from 0.65 to 0.80. The net gain or loss of latent heat flux Q_E is small on account of vapor pressure near the value at the glacier surface. Heat loss by net longwave radiation Q_L was large, since radiation from the clouds was small due to low cloud amount. Therefore, heat gain by net radiation $Q_N (= Q_S + Q_L)$ is small (mean, 66 cal·cm⁻²); accordingly the sensible heat flux (mean, 27 cal·cm⁻²) is at a significant level. The negative value of Q_W reveals that the heat used to warm the surface layer was larger than heat release due to cooling. The surface layer is cooled down to temperature far below 0°C at night, and much heat is required to raise its temperature to 0°C in the daytime, which results in a low percentage of heat available for the melting process Q_M . As a result, the average daily snowmelt during these 7 days was less than 0.5 cm in water equivalent. The absolute value of the heat gain is not so large, presumably because of the reduction of incoming solar radiation in the afternoon when the orographic clouds were formed. The general tendency of excessive heat gain in relation to the heat loss (within 17%) may be partially due to underestimation of heating in the surface layer, since it was calculated from temperature at 4 depths in this layer, but no data were available below the depth of 40 cm.

Table 1. Mean values of heat balance components (cal·cm⁻²) at the glacier surface.

	Q_S	Q_L	Q_H	Q_E	Q_W	Q_M	Mean heat gain	Mean heat loss
Daytime balance	135	-69	27	-2	-54	-20	162	-145
Daily balance	131	-153	46	-9	-15	-19	177	-196

Daytime balance: mean values for September 29–October 1 and October 12–15 (06:00–18:00). Daily balance: mean values for October 12 06:00–16 06:00. Mean heat gain represents the sum of each positive component; mean heat loss the sum of each negative component.

As seen in Table 1, the mean heat gain in the daytime was in fairly good agreement with the mean heat loss in the daytime. Since each component of heat balance was determined independently, it can be said from such agreement that the method of calculation of heat balance was valid in the daytime. For more accurate estimation of the heat balance, the effect of latent heat release associated with refreezing of meltwater also needs to be investigated.

5.3. Daily heat balance

As seen in Table 1, large heat loss due to net longwave radiation is the most significant feature in the daily heat balance. Consequently, the amount of net radiation became negative ($-22 \text{ cal}\cdot\text{cm}^{-2}$), which was compensated by the heat supply due to sensible heat flux ($46 \text{ cal}\cdot\text{cm}^{-2}$). The low value of Q_W means that the heating in the daytime and the cooling at night were nearly balanced throughout the day in the surface layer.

It is also shown that the estimated value of heat gain is about $20 \text{ cal}\cdot\text{cm}^{-2}$ smaller than that of heat loss in the case of the daily heat balance. One of the reasons for this disagreement may be the method of calculation used, which excludes the contribution of heat gain associated with refreezing of meltwater which remained in the snow cover. In addition, the sensible heat flux might be underestimated due to the characteristic profile of the katabatic wind which shows a steep wind and temperature gradient near the surface.

5.4. Diurnal variation of main components of heat balance

In Fig. 6, a typical example of the diurnal variation of net radiation Q_N and sensible heat flux Q_H during the period October 13 06:00–14 18:00 is shown by hourly mean values. The air temperature at 0.8 m level, $T_{0.8}$, the difference of air temperature in the first 0.8 m above the glacier surface, ΔT_1 , the wind speed at 1.1 m level, $u_{1.1}$ and the wind direction are also shown in Fig. 6. Q_N was nearly $-0.12 \text{ cal}\cdot\text{cm}^{-2}\cdot\text{min}^{-1}$ during a long period at night. This is a reason for the negative value of Q_N in daily heat balance. In contrast, Q_H was always posi-

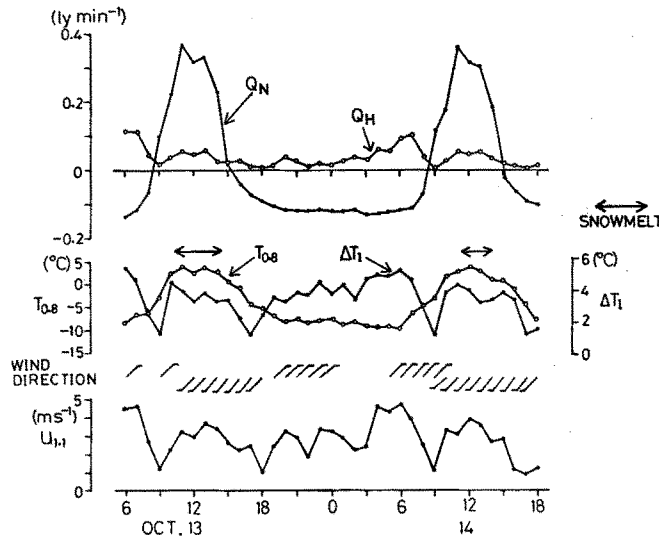


Fig. 6. Daily course of main components of heat balance at the glacier surface, air temperature at 0.8 m level, temperature difference between 0.8 m level and the glacier surface, wind speed at 1.1 m level and wind direction. The periods when snowmelt occurred are also shown. See text for details.

tive with the maximum of nearly $0.1 \text{ cal}\cdot\text{cm}^{-2}\cdot\text{min}^{-1}$ at around 06:00. This maximum can be explained by the maximum of the temperature difference ΔT_1 and the maximum of the wind speed $u_{1,1}$ reaching $5 \text{ m}\cdot\text{s}^{-1}$, when a katabatic wind occurred. Therefore it would be reasonable to consider that the large sensible heat flux in this case is due to the strong temperature inversion which occurred immediately before the sunrise and the snowmelt period and the great speed of the katabatic wind. The inversion in the daytime can be explained by horizontal advection of warm air, as will be discussed in the next section.

6. Effect of warm air advection from snow-free area on temperature profile above glacier surface

The profile of air temperature above the glacier surface is essential for estimating the sensible heat flux at the glacier surface. Major factors in controlling the temperature profile are the change of radiative heat balance at the surface and the local advection. Since the observation site M is at a distance of only 70 m from the glacier ice margin, the temperature profile can be strongly affected by the warm air advection from the snow-free area (Treidl, 1970; Weisman, 1977; Riordan, 1982). Such an effect was studied by simultaneous observations on melting of newly fallen snow at site P 30 m away from the glacier ice margin at the moraine, air temperature and surface temperature at the sites M and P. The observation period was from October 17 to 21.

The ground was free from snow on October 17. A snowfall occurred on October 18, lowering the snow line to the elevation of about 4600 m. After that the weather recovered but the snow cover remained until October 21. Considerable compaction of the snow occurred on October 19. The winds were SW, namely, from the ground onto the glacier, throughout the daytime during the observation period.

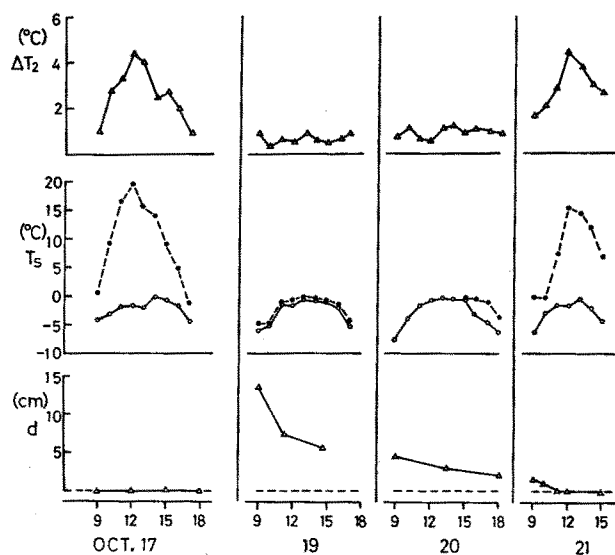


Fig. 7. Effect of warm air advection from the snow-free area on the temperature inversion above the glacier surface at site M. Snowfall occurred on October 18.

ΔT_2 : temperature difference between 0.4 m level and the glacier surface

T_s : surface temperature (open circle; site M, solid circle; site P)

d : snow depth at site P

Fig. 7 shows snow depth (d), hourly values of surface temperatures (T_S) at sites M and P, and temperature difference (ΔT_2) between 0.4 m level ($T_{0.4}$) and the glacier surface, i.e., $\Delta T_2 = T_{0.4} - T_S$, at site M in the daytime before and after the snowfall. It is obvious that ΔT_2 has a strong dependency on the difference of surface temperature between the sites M and P.

Before the snowfall period the ground was intensively heated to a maximum temperature of 20°C, resulting in a great difference of surface temperature between the glacier and the ground. Under this condition ΔT_2 increased to 4.5°C at site M. When the ground was covered with snow to a large extent, the difference of surface temperatures was reduced almost to zero, and ΔT_2 was reduced to within 1°C (October 19). When snow cover became thin (in the afternoon on October 20), the ground at site P was prevented from cooling until just before sunset, due to the decreasing albedo of the snow surface and the increasing influence of the sensible heat supply from the sporadic snow-free areas (Holmgren et al., 1975; Inoue and Yasunari, 1984). However, ΔT_2 was still small. When the ground surface appeared, ΔT_2 showed a rapid increase with increasing difference of surface temperatures (October 21). During this observation period radiative cooling did not occur except near sunset, so it would be reasonable to consider that advection played a primary role in controlling surface inversion at site M.

Fig. 8 shows typical profiles of the air temperature at sites M and P with and without snow cover. Wind speed at the 1.1 m level was nearly 3 m·s⁻¹ in both cases. Under the snow-free condition at the ground surface (11:30 on October 17) a marked contrast existed between the air temperatures above the glacier and the ground surface. Furthermore, the temperature difference in the first 0.4 m above the glacier surface, ΔT_2 , reached 4.3°C. When the ground was covered with snow (11:30 on October 19), temperature profiles at both sites resembled each other and ΔT_2 decreased to 0.8°C.

Such a difference can be explained in the light of air-mass modification. In the snow-free condition at site P, there is a discontinuity in surface temperature at the glacier ice margin, and substantial modification of air mass will take place especially near the glacier surface within twenty or thirty meters of the glacier ice margin. Conversely, when the ground is covered with snow, the air mass must travel a long distance over the snow surface to reach the glacier. As a result, the air mass is nearly in temperature equilibrium with the underlying snow surface, and the vertical temperature gradient is near zero in the lower part of the boundary layer at sites P and M.

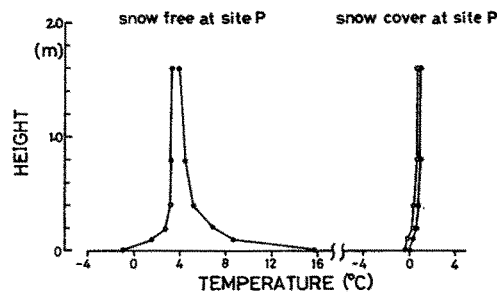


Fig. 8. Vertical profiles of air temperature at sites M (open circle) on the glacier and P (solid circle) on the ground. (left) Snow-free condition at site P (October 17, 11:30). (right) Snow-covered condition at site P (October 19, 11:30).

On the basis of such considerations the sensible heat flux at the glacier surface can be expected to be small at the central part of the glacier.

7. Concluding remarks

As described in the foregoing, the primary heat source in the daytime was net shortwave radiation accounting for 83% (135 cal·cm⁻²) of the heat gain, and the remaining took the form of sensible heat flux 17% (27 cal·cm⁻²). Reflecting the less cloudy condition especially at night, the daily net radiation became negative (−22 cal·cm⁻²), which was compensated by sensible heat flux (46 cal·cm⁻²). In spite of the cool weather, such values of sensible heat flux are several times as large as the result obtained by Ohata and Higuchi (1980) during the summer monsoon season in Shorong Himal, Nepal. The different wind speed can partially account for this contradiction; the mean value is 3.1 m·s⁻¹ in this study and 1.2 m·s⁻¹ in Shorong Himal. However, it can be more clearly understood in terms of the strong katabatic wind and the warm air advection from the snow-free area dominating the process of sensible heat transfer. This would be considered as an indication that the sensible heat flux at the glacier surface is largely affected by local climatic conditions. Local climatic conditions also play a part in controlling the radiative balance by the formation of orographic clouds. These facts are considered as important characteristics of heat balance at the glacier surface during the post-monsoon season, in the high Himalaya.

More research needs to be done on the thermal effect of bare ground upon heat transfer at the glacier in connection with the areal or regional distribution of heat sources and heat sinks, as a means to understand more clearly the regional heat regime in the high Himalaya.

References

- Bradley, E. F. (1968): A micrometeorological study of velocity profiles and surface drag in the region modified by a change in surface roughness. *Quart. J. Roy. Met. Soc.*, 94, 361–379.
- Hoinkes, H. (1954): Der Einfluss des Gletscherwindes auf die Ablation. *Zeitschrift für Gletscherkunde und Glaziologie*, Bd. 3, 18–23.
- Hoinkes, H. (1955): Beiträge zur Kenntnis des Gletscherwindes. *Arch. Meteor. Geophys. Biokl.*, Ser. B6, 36–53.
- Holmgren, B., Benson, C. and Weller, G. (1975): A study of the breakup on the Arctic slope of Alaska by ground, air and satellite observations. *Climate of the Arctic*, Geophysical Institute, University of Alaska, 358–366.
- Inoue, J. and Yoshida, M. (1980): Ablation and heat exchange over the Khumbu Glacier. *Seppyo*, 41, Special Issue, 26–33.
- Inoue, J. and Yasunari, T. (1984): Surface heat exchange in the high Himalayas. (To be published).
- Munro, D. S. and Davies, J. A. (1977): An experimental study of the glacier boundary layer over melting ice. *J. Glaciology*, 18, 425–436.
- Ohata, T. and Higuchi, K. (1979): Gravity wind on a snow patch. *J. Met. Soc. Japan*, 57, 254–263.
- Ohata, T. and Higuchi, K. (1980): Heat balance study on Glacier AX010 in Shorong Himal, East Nepal. *Seppyo*, 41, Special Issue, 42–47.
- Rao, K. S., Wyngaard, J. C. and Coté, O. R. (1974): The structure of the two-dimensional internal boundary layer over a sudden change of surface roughness. *J. Atmos. Sci.*, 31, 738–746.
- Riordan, A. J. (1982): Formulation and testing of a climatonic simulation of the microclimate of the dry valleys and of the Little America V Station in Antarctica. *Boundary Layer Meteorol.*, 24, 295–329.
- Treidl, R. A. (1970): A case study of warm air advection over a melting snow surface. *Boundary Layer Meteorol.*, 1, 155–168.

- Webb, E. K. (1970): Profile relationships: the log-linear range, and extension to strong stability. *Quart. J. Roy. Met. Soc.*, 96, 67–90.
- Weisman, R. N. (1977): Snowmelt: a two-dimensional turbulent diffusion model. *Water Resour. Res.*, 13, 337–342.
- Yamada, T., Motoyama, H. and Thapa, K. B. (1984): Role of glacier meltwater in discharge from the glaciated watersheds of Langtang Valley, Nepal Himalaya. in this issue.
- Yasunari, T. (1980): Air-borne measurements of the surface temperature over the Nepal Himalayas. *Seppyo*, 41, Special Issue, 82–85.